

In this Issue

Articles

Inter Comparison of GIRO predictions with VIIRS DNB Observations over DCC targets.

By Changyong Cao, NOAA

AIRS Calibration Update and Radiometric Uncertainty Estimate

By T. Pagano, H H Aumann, S Broberg, E Manning, J Teixeira (JPL), K Overoye (BAE Systems) and L Strow (UMBC)

Lunar Observation Planning for LEO Satellite Instruments

By Truman Wilson (SSAI) and Xiaoxiong (Jack) Xiong (NASA)

GSICS Use of GRUAN Humidity Observations in the context of Satellite Sensor Assessment

By Bomin Sun (NOAA), Xavier Calbet (AEMET), Tony Reale (NOAA) and Manik Bali (NOAA)

News in This Quarter

GSICS 20th Executive Panel Meeting (EP 20) held in Sochi, Russia

By Mitch Goldberg (NOAA), Kenneth Holmlund (EUMETSAT), Toshi Kurino (WMO), Lawrence Flynn (NOAA), Manik Bali (NOAA), Dohyeong Kim (KMA), Masaya Takahashi (JMA) and Alexey Rublev (ROSHYDROMET)

Toshiyuki Kurino Bids Adieu to GSICS

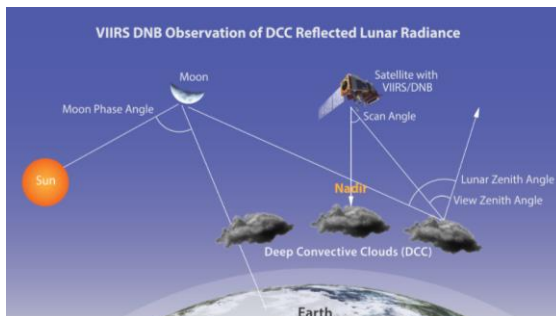
By Manik Bali, GSICS Coordination Center

Announcements

COSMIC-2 Launched on 25 June, 2019

By Shu Peng (Ben) Ho and Manik Bali, NOAA

GSICS Related Publications



The Image above depicts GIRO-VIIRS inter-comparisons using DCC targets



Information on GSICS IR References AIRS, IASI and CrIS

Inter-Comparison of GIRO predictions with VIIRS DNB Observations over DCC targets

By Changyong Cao, NOAA

In a recent study published in the journal Remote Sensing titled “Radiometric Inter-Consistency of VIIRS DNB on Suomi NPP and NOAA-20 from Observations of Reflected Lunar Lights over Deep Convective Clouds” by Changyong Cao, Yan Bai,

Wenhui Wang, and Jason Choi

(available online at:

<https://doi.org/10.3390/rs11080934>),

it was found that the lunar radiances observed by the VIIRS DNB are consistent with GIRO predictions within 3%. This study presented a novel method for evaluating the observation consistency and accuracy between VIIRS DNB on two or more satellites. The method is a valuable tool for the routine data quality monitoring and evaluation of NOAA operationally produced data for users worldwide. It takes advantage of the faint reflected lunar light at night from the deep convective clouds to perform the data quality assessments, in conjunction with the latest lunar irradiance model developed under the Global Space-based Inter-calibration System (GSICS).

The study compared nighttime Suomi NPP and NOAA-20 VIIRS DNB measured DCC reflected lunar radiance at various phase angles using data from July 2018 to March 2019 with an 86 second sampling interval, and compared Suomi NPP VIIRS DNB measured lunar radiances with those from the GIRO lunar model predictions. It was found that observed lunar radiance from VIIRS DNB on Suomi NPP to be consistent with GIRO model predictions within $3\% \pm 5\%$ (1σ) for a large range of lunar phase angles. However, discrepancies are significant near full moon, due to lunar opposition effects, and limitations of the GIRO lunar model. Also, the result shows good consistency between the VIIRS DNB instruments on the two satellites, which significantly outperforms the

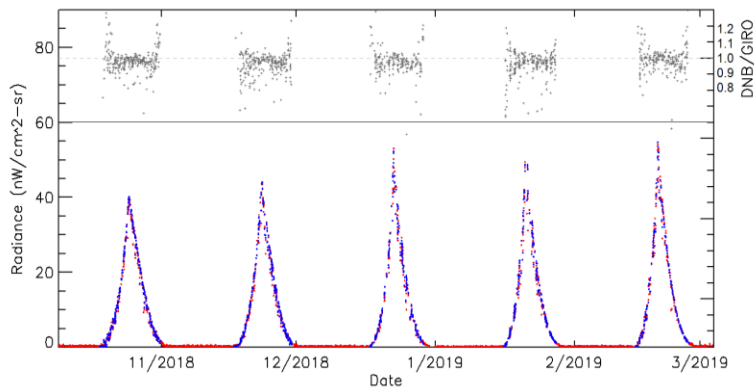


Figure 1. Time series of Suomi NPP VIIRS DNB measured reflected lunar radiance over DCC compared with GIRO predicted values (low panel: radiance comparison; up panel: radiance ratio DNB/GIRO)

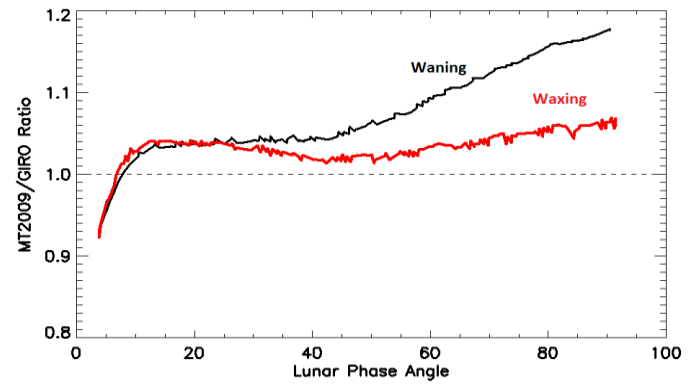


Figure 2. Comparison between GIRO and MT2009 predicted lunar irradiance

mission requirement, although a low bias in the NOAA-20 VIIRS DNB of ~5% is found. In addition, the study also compared the model predicted lunar irradiance from two models: the GIRO and MT2009 (by Miller and Turner, 2009). The results show that these two models produced relatively consistent results, although the differences grow up to 17% with increasing lunar phase angle (Figure 2). Differences are also found between waning and waxing phases of the

moon.

The study is useful not only for monitoring the DNB calibration stability and consistency across satellites, but also may help validate lunar models independently. The VIIRS DNB has been used for a variety of applications including geophysical retrievals of clouds, aerosols, aurora, and air glows, as well as social economic studies including power outage due to severe weather,

emergency response, and the correlation of night light with economic growth, population, and infrastructure. The good consistency between VIIRS DNB on different satellites, and with lunar models benefits the users who study the time series of night lights for a variety of applications. This study also exemplifies the benefits of the GIRO as an interagency collaboration effort under the WMO GSICS.

[Discuss the Article](#)

AIRS Calibration Update and Radiometric Uncertainty Estimate

By Thomas S. Pagano, Hartmut H. Aumann, Steve Broberg, Evan Manning, Joao Teixeira, (JPL), Kenneth Overoye, (BAE Systems) and Larrabee Strow (UMBC)

1. The Atmospheric Infrared Sounder (AIRS) on Aqua

The Atmospheric Infrared Sounder (AIRS) is a “facility” instrument developed by NASA as an experimental demonstration of advanced technology for remote sensing and the benefits of high resolution infrared spectra to science investigations¹. It was launched into polar orbit on May 4, 2002 on the EOS Aqua Spacecraft, and is expected to

provide data beyond 2024. AIRS has 2378 infrared channels ranging from 3.7 μm to 15.4 μm and a 13.5 km footprint. The AIRS data are used for weather forecasting, climate process studies and validating climate models². For more information see <http://airs.jpl.nasa.gov>. AIRS is a vital IR reference sensor for GSICS and is used by JMA for comparison to Himawari 8/9 AHI³, KMA for comparison to COMS⁴, NOAA for comparison to CRIS⁵ and GOES-ABI⁶,

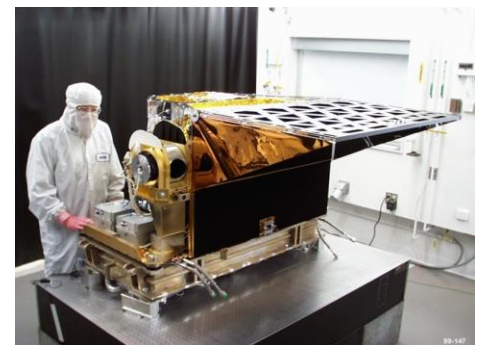


Figure.1. Atmospheric Infrared Sounder at developer BAE Systems.

and EUMETSAT for comparison to IASI⁷.

The AIRS instrument (Figure 1), developed by BAE SYSTEMS, incorporates numerous advances in infrared sensing technology to achieve a high level of measurement sensitivity, precision, and accuracy. This includes a temperature-controlled spectrometer (157K) and long-wavelength cutoff HgCdTe infrared detectors cooled by an active-pulse-tube cryogenic cooler. It is this temperature control that is most likely responsible for the observed stability in the instrument. The Focal Plane Assembly (FPA) contains 12 modules with 15 individual PV HgCdTe line arrays of detectors in a 2 x N element arrays where N ranges from 94 to 192 for PV HgCdTe, and 2 PC HgCdTe arrays with 1 x 144, 1 x 130 elements. The AIRS acquires 2378 spectral samples at resolutions, $\lambda/\Delta\lambda$, ranging from 1086 to 1570, in three bands: 3.75 μm to 4.61 μm , 6.20 μm to 8.22 μm , and 8.8 μm to 15.4 μm . AIRS scans the Earth scene up to $\pm 49.5^\circ$ relative to nadir with a spatial resolution of 13.5 km. Each scan provides a full-aperture view of space and an on-board blackbody calibration source. The key to the high accuracy and NIST traceability of AIRS is the high quality full aperture On-Board Calibrator (OBC) blackbody and 4 full aperture space views. The OBC is a specular coated wedge design with an internal angle of 27.25° .

2. Radiance Data Products

The AIRS Level 1B algorithm converts digital counts to calibrated radiances⁸. The radiances follow a second order polynomial in signal difference between the earth view signals and space view signals. The gain term is updated every granule (6 minutes) using the on-board blackbody and space view as a two point calibration. The offset is computed using a model

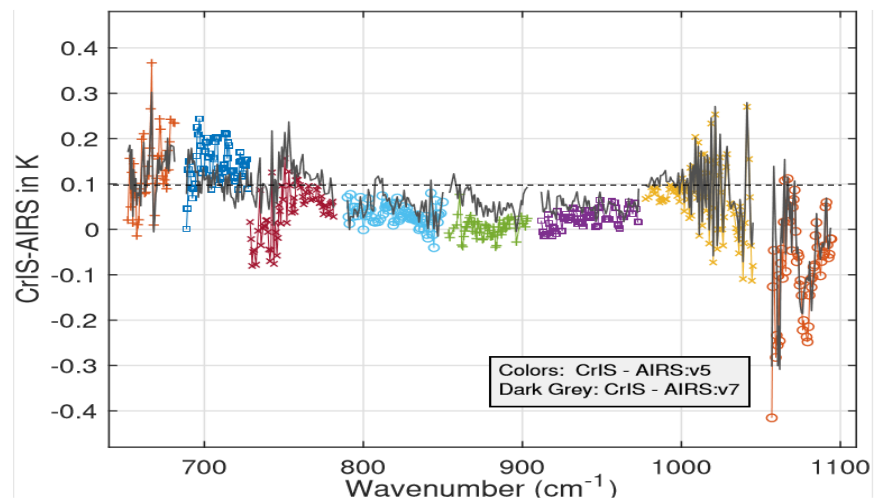


Figure 2. CrIS-AIRS shows less module-to-module variability in the AIRS:v7 than AIRS:v5. A 0.1K bias between the two instruments is becoming apparent

of the instrument emission based on polarization factors of the scan mirror and spectrometer, and mirror temperature. The nonlinear term is based on pre-flight measurements. The radiometric calibration pre-flight involves measuring the polarization parameters, blackbody effective emissivity and temperature, and response nonlinearity. The computed radiances, diagnostic, and QC information are provided in the AIRS Level 1B product.

The excellent radiometric stability of the AIRS is discussed in several prior publications⁹. Comparison of AIRS brightness temperatures with sea surface temperatures from the NOAA floating buoy network measured under clear non-frozen ocean conditions shows less than 10 mK/year drift. The AIRS spectrum is calibrated using spectral absorption features in the upwelling spectrum. At present, we have shown the ability to both calibrate to better than 1 ppm and correct the spectra for time varying spectral calibration including Doppler corrections¹⁰. These corrections along with cleaned and gap filled radiances (using PC reconstruction) will be available in a new Level 1C product expected to be public later this year. For the Level 1B, spectral calibration

data are provided separately in calibration properties files by epoch. More information is found in the AIRS Level 1B user guide¹¹.

3. AIRS Radiance Data Product Improvements

The AIRS Version 5 coefficients were sufficiently accurate that an update has never been made since AIRS launch in 2002. Significant progress has been made to improve the accuracy of the AIRS radiances¹². An update to the radiometric calibration coefficients is under review for Version 7. The new set is based on new measurements in space or a better understanding of data obtained pre-flight. First we re-derive the radiometric calibration equation with a little more rigor and account for the view angle of each of the 4 space views. Second, new polarization coefficients are derived from the 4 space views covered in the instrument; they range from 83° - 101° . Third, the effective blackbody emissivity is smoothed after determining that the spectral structure seen in pre-flight testing may have been test related. Fourth, separate nonlinearity coefficients are used for the A and B sides of the AIRS channels rather than AB averages, based on the re-analysis of pre-flight data. As shown in Figure

3, when we compare to the CrIS, that better agreement is made in Version 7. We can start to see now a constant bias between AIRS and CrIS of 0.1K. We also see a general improvement in Left/Right Asymmetry when observing deep convective clouds. The impact of the new coefficients is highest at coldest scene temperatures.

The radiometric accuracy for AIRS can be determined by combining the error contributions from all the terms in the radiometric transfer equation (conversion of counts to radiance). The 1-sigma temperature uncertainty for AIRS Version is better than 0.15 K for all channels in Version 7¹³. Results for Version 5 are only slightly poorer with up to 0.1K higher in some channels. The dominant error to the calibration accuracy is the nonlinearity followed by the polarization phase and OBC temperature. Results for the current Version 5 have been submitted for inclusion in the Global Space-based Inter-Calibration System report "Traceability and Uncertainty of GSICS Infrared Reference Sensors".

4. Summary and Conclusions

The AIRS radiometric calibration is so straightforward that an update has not been required since AIRS launch in 2002. Currently the Version 5 Level 1B is available, but an update (Version 7) is expected to be available in mid-2020. The high accuracy and stability of AIRS makes the data valuable for weather forecasting and climate research. The continuous more than 20-year long AIRS data record available at the end of mission will be

an extremely valuable tool for studies of the changing climate in this critical time in history.

ACKNOWLEDGEMENTS

The research was carried out at the Jet Propulsion Laboratory, California Institute of Technology, under a contract with the National Aeronautics and Space Administration. © 2019. All rights reserved.

Bibliography

- [1] Pagano, T.S, et al., Standard and Research Products from the AIRS and AMSU on the EOS Aqua Spacecraft, Proc. SPIE Vol. 5890, p. 174-183
- [2] J. LeMarshall, J. Jung, J. Derber, R. Treadon, S. Lord, M. Goldberg, W. Wolf, H. Liu, J. Joiner, J. Woollen, R. Todling, R. Gelaro Impact of Atmospheric Infrared Sounder Observations on Weather Forecasts, EOS, Transactions, American Geophysical Union, Vol. 86 No. 11, March 15, 2005
- [3] https://www.data.jma.go.jp/mscweb/data/monitoring/gsics/ir/monit_g_eoleoir.html
- [4] <http://nmsc.kma.go.kr/html/homepage/en/gsics/Infrared/gsicsIrTimeSequence.do>
- [5] Tobin, D., et al. (2013), Suomi-NPP CrIS radiometric calibration uncertainty, J. Geophys. Res. Atmos., 118,10,58910,600, doi:10.1002/jgrd.50809.
- [6] <https://www.star.nesdis.noaa.gov/smcd/GCC/ProductCatalog.php>
- [7] Hilton, F. et al., "Hyperspectral Earth Observation from IASI: four years of accomplishments", BAMS

(2011), doi: 10.1175/BAMS-D-11-00027.1

- [8] Pagano, T., H. Aumann, D. Hagan, K. Overoye, "Pre-Launch and In-flight Radiometric Calibration of the Atmospheric Infrared Sounder (AIRS)", IEEE TGRS, 41, No. 2, Feb. 2003, p. 265.
- [9] Hartmut H. Aumann, Evan M. Manning, Steve Broberg, "Radiometric stability in 16 years of AIRS hyperspectral infrared data," Proc. SPIE 10764, Earth Observing Systems XXIII, 1076400 (7 September 2018); doi: 10.1117/12.2320727
- [10] Strow, L. L., S. E. Hannon, S. De-Souza Machado, H. E. Motteler, and D. C. Tobin (2006), "Validation of the Atmospheric Infrared Sounder radiative transfer algorithm", J. Geophys. Res., 111, D09S06, doi:10.1029/2005JD006146
- [11] https://docserv01.gesdisc.eosdis.nasa.gov/repository/Mission/AIRS/3.3_ScienceDataProductDocumentation/3.3.4_ProductGenerationAlgorithms/V5_L1B_QA_QuickStart.pdf
- [12] Pagano, T., Broberg, S., Manning, E., Aumann, H., Strow, L., Weiler, M., "Reducing uncertainty in the AIRS radiometric calibration", Proc. SPIE, 10764-23, August 2018
- [13] Pagano, T. S. et al., "Updates to the Absolute Radiometric Accuracy of the AIRS on Aqua", Proc. SPIE 10781-26, Honolulu, HI (2018)

[Discuss the Article](#)

Lunar Observation Planning for LEO Satellite Instruments

By Truman Wilson (SSAI) and Xiaoxiong(Jack) Xiong (NASA)

Introduction

The Moon has been an important source for monitoring the radiometric stability of Earth-observing instruments on satellites in low-Earth orbit. For many instruments, such as MODIS on-board the Terra and Aqua platforms and VIIRS on-board the Suomi-NPP and NOAA-20 platforms, instrument maneuvers are required in order to bring the Moon into view in the desired phase angle range [1, 2]. This phase angle range restriction helps to constrain the geometric correction factors that are applied from the USGS ROLO model, allowing for better comparisons of the radiometric gain between separate observations [3].

For most instruments, maneuvers will generally be restricted about specific axes based on the location of the maneuvering thrusters and also restricted to specific ranges for instrument safety reasons. For mission planning purposes, it is important to understand the availability of observations given these constraints and to choose a parameter range that will allow for frequent and long-term radiometric monitoring. Since each

mission may have different restrictions, it is important to have a tool that is flexible for planning observations. For this purpose, we have developed a lunar observation planning tool which we can use to determine the timing of observations for spacecraft maneuvers and view-ports along arbitrary axes [4]. For MODIS and VIIRS, regularly scheduled lunar observations use a roll maneuver and view the Moon through the instrument space-view port. They can also use instrument pitch maneuvers to view the Moon at an arbitrary angle through the Earth-view port. The methodology developed here can also be easily extended for determining the observation times of the sun, planets, stars, and Earth-view overpasses of a selected target by the satellite at specified view-angles.

Methodology

To facilitate the development of this tool, we relied on the SPICE Toolkit developed by NASA's Navigation and Ancillary Information Facility at the Jet Propulsion Laboratory, particularly the Geometry Finder (GF) tool. We currently use DE430 for the ephemeris data for the

solar system bodies, and Two-Line Element sets from CelesTrak for the satellite orbital data. Instrument and observation reference frames can be defined in the form of time-dependent SPICE kernels which will allow us to compute the position of the desired target in the reference frame at an arbitrary time.

The instrument coordinate system (ICS) is defined with nadir along the z -axis, the x -axis along the direction of satellite motion (perpendicular to z), with the y -axis normal to the instrument orbital plane, as seen in Figure 1(a). The ICS can be defined in SPICE in either a geocentric (MODIS) or geodetic (VIIRS) configuration. The observation coordinate system (OCS) has a fixed offset relative to the ICS. The OCS z' -axis will be aligned with the instrument maneuvering axis, R . The OCS is further rotated such that the viewport, V , is in the OCS $x'z'$ -plane, as seen in Figure 1(b). When the spacecraft rotates, the viewport will sweep out a cone of observation in the OCS. If we choose latitudinal coordinates for the OCS, an observation will be possible when the target, T , is at the same latitude in the

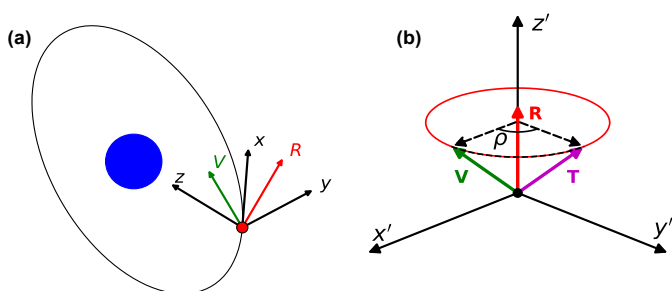


Figure 1: (a) Definition of the ICS with the rotation (R) and viewport (V) axes shown. (b) The OCS showing an instrument manoeuvre to align the viewport with the target (T).

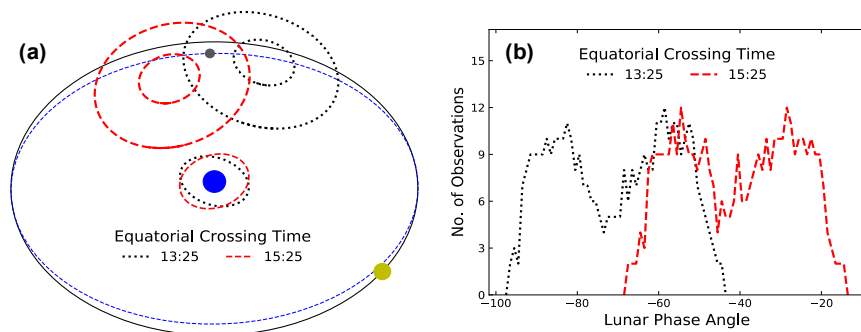


Figure 2: (a) Orbit diagram for two equatorial crossing times with the corresponding fields-of-view projected on the Moon orbit. (b) Histograms for 1 year of lunar observations as a function of phase angle in 1-degree bins

Table 1: Example pitch observation predictions. (D) and (A) represent descending and ascending daytime orbits, respectively. The observations at the three view angles can span multiple days.

Instrument Eq. Crossing Obs. Date		Lunar Phase	@	View Angle	
		-15°	0°	+15°	
Terra MODIS	09:30 (D)	July 2, 2020	-18	-33	-50
Terra MODIS	10:00 (D)	July 3, 2020	-10	-26	-42
Terra MODIS	10:30 (D)	July 3, 2020	-3	-19	-34
Aqua MODIS	13:35 (A)	July 6, 2020	2	18	33
SNPP/N20 VIIRS	13:25 (A)	July 6, 2020	-1	15	31

OCS as the viewport. The longitudinal offset is the required rotation angle for the observation, ρ . To find the observation times, we can use the GF to apply a set of constraints which can be used to do phase angle selection, maneuver restrictions, and target latitude checks. In principle, an arbitrary number of geometric restrictions can be applied using the GF to filter the observation results.

Orbit Simulations

Using simulated orbital data, we can use this tool to perform simulations of lunar observations for different instrument conditions. As an example, in Figure 2(a), we show the relative orbital geometry for VIIRS-like instruments at different equatorial crossing times. The possible fields-of-view for the space-view port with maneuvers are shown by the circles for each orbit. A histogram of the number of potential lunar observations as a function of phase angle for 1 year of simulated orbits is shown in Figure 2(b).

Another simulation can be performed in order to predict future pitch maneuver observation opportunities (about the ICS y -axis) for MODIS and VIIRS instruments. In this case, the spacecraft rotation and lunar phase angle restrictions are removed, and we restrict the observations to occur within the first quarter spacecraft night for instrument safety reasons. Since the observations occur in the EV port, a number of view angles are possible during the observations. Some of these parameters are listed in Table 1. In Table 1, we also showed predictions for earlier equatorial crossing times for Terra MODIS, which will be allowed to drift from its current orbit in the coming years.

Summary

We developed a lunar observation planner that can be used for instruments with arbitrary maneuvering and viewport axes. Using simulated orbital data, we can determine the available observation opportunities which can be used for future mission planning. The tool can also be extended to finding

observation times for arbitrary targets, including the Sun, bright planets, stars, and Earth-view targets.

References

- [1] J. Sun, X. Xiong, W. Barnes, and B. Guenther, "MODIS reflective solar bands on-orbit lunar calibration," *IEEE Trans. Geosci. Remote Sens.*, vol. 45, no. 7, p. 2383, 2007.
- [2] X. Xiong, J. Sun, J. Fulbright, Z. Wang, and J. Butler, "Lunar calibration and performance for S-NPP VIIRS reflective solar bands," *IEEE Trans. Geosci. Remote Sens.*, vol. 54, no. 2, p. 1052, 2016.
- [3] H. H. Kieffer and T. C. Stone, "The spectral irradiance of the Moon," *Astron. J.*, vol. 129, no. 6, pp. 28872901, 2005.
- [4] T. Wilson and X. Xiong, "Planning lunar observations for satellite missions in low-Earth orbit," *J. Appl. Remote Sens.*, vol. 13, no. 2, p. 024513, 2019.

[Discuss the Article](#)

GSICS Use of GRUAN Humidity Observations in the context of Satellite Sensor Assessment

By Bomin Sun (NOAA), Xavier Calbet (AEMET), Tony Reale (NOAA), and Manik Bali (NOAA)

The Global Climate Observing System (GCOS) Reference Upper Air Network (GRUAN) is an international observing network, designed to provide reference, atmospheric (geophysical) observations to fill “gaps” in the current WMO Integrated Global Observing System (WIGOS). GRUAN currently consists of about 20 active sites and at least 10 more under consideration for certification. GRUAN is evolving and envisioned as a network of about 40 sites. Meanwhile, the current observations provide reasonable to good global coverage of value in emerging satellite product calibration/validation (cal/val) including for calibrated radiance. The Global Space-based Inter-Calibration (GSICS) recently (2017) undertook actions to demonstrate the use of GRUAN radiosondes to support ongoing monitoring of observed (calibrated) radiometric spectra from the various environmental satellites. The following article tracks one such action focused on impacts in satellite hyperspectral IR spectra of expected differences (improvements) in radiosonde moisture measurement technology; a difficult task in the IR where clouds contaminate. Results address impacts in both the radiance and geophysical space.

Calbet et al. (2017) originally found that GRUAN RS92 nighttime observations are consistent with Infrared Atmospheric Sounding Interferometer (IASI) measurements in the upper tropospheric water vapor absorption spectrum. They noticed this, after accounting for the

uncertainties of GRUAN and Infrared Atmospheric Sounding Interferometer (IASI) measurements and the time and space collocation mismatch between the radiosonde and IASI pixel. That work signaled that GRUAN data can be utilized to supplement GSICS in the monitoring and assessment of environmental satellite sensors.

Similar to other long-term observing systems, upper-air instrumentations migrate (advance) over time. Vaisala RS41 has been replacing the Vaisala RS92 in the past several years, becoming the major sonde type across the GRUAN sites (and conventional radiosonde network). Characterizing the measurement improvement (and accuracy) of this emerging radiosonde type is key to the GRUAN RS92-to-RS41 transition management program. It is also of interest to upper-air climate trend detection, NWP data assimilation and (through GSICS) the satellite cal/val community.

The assessment of GRUAN RS92 humidity observations by Calbet et al. (2017) was conducted in radiance space, and this study uses the same approach. Basically, radiance is computed in the upper tropospheric water vapor absorption band (1400-1900 cm^{-1}) from a radiosonde temperature and humidity profile using the Line-by-Line Radiative Transfer Model (LBLRTM, Clough et al. 2005). Then, collocated IASI measurements are compared with the computed radiosonde radiances to find out if the two types of measurements are consistent with each other. IASI and

radiosonde data are considered to be consistent with each other if their difference in radiance is within 2 times (i.e., $k = 2$) the standard error. As described by Immler et al. (2010), with normally distributed variables and independent uncertainty factors, the standard error is the square root of the ($\sigma^2 + u_1^2 + u_2^2$) term described in the following equation.

$$|m_1 - m_2| < k \sqrt{\sigma^2 + u_1^2 + u_2^2}$$

where “ m_1 ” and “ m_2 ” are two radiance measurements to be compared, “ u_1 ” and “ u_2 ” the associated uncertainties, “ σ ” the uncertainty due to mismatch and “ k ” the agreement parameter. This is a 2-sided test of consistency at approximately the 95% statistical significance level.

A key to this assessment is that IASI pixels collocated with radiosondes should be cloud free to guarantee that the infrared radiance being compared is not cloud contaminated. Undetected high clouds, present in the “cloud-free” scenes identified in this study would bias the assessment. Caution is therefore needed to identify cloud-free scenes. Additionally, use of closely collocated radiosonde-satellite pairs reduces random atmospheric variability from the assessments, which can exceed the magnitude than the uncertainties of the radiosonde and IASI instruments (Calbet et al., 2017). However, tight time windows (even under clear sky) are no guarantee and highly homogeneous atmospheric cases separated by several hours (and km’s) can lead to $k=2$ (even 1).

In this study, RS92-RS41 dual launches (both radiosondes attached to the same balloon) at Lauder, New Zealand, a GRUAN site, are used as the example to understand the difference and improvement of RS41 from RS92 in the upper tropospheric humidity observations. Lauder, New Zealand is one of a few GRUAN sites with launches made at synoptic times mostly within 1hr before MetOp overpass. Most of the sondes launched at the site, however, are during daytime (at local time around 9:00 am). So, the analysis is limited to 16 daytime launches with “cloud-free” scenes identified using the cloud information included in the EUMETSAT IASI L2 product. Soundings and IASI collocations are within 1 hr and 50 km.

Currently, the GRUAN Data Processing (GDP, Dirksen et al. 2014) is the version 2 for the Vaisala RS92 and still under development for RS41. Therefore, RS92 and RS41 profiles in dual flights at Lauder are combined GDP and manufacturer-processed data, respectively. Both soundings are originally in 1-s vertical resolution and are converted into “standard” 100 vertical layers for use in RTM radiance computation.

Figure 1 shows the mean difference between IASI observed and calculated radiance averaged from the 16 daytime cloud free scenes for RS92 (top) and RS41 (middle) dual launches from Lauder. The negative OBS-CAL differences shown for both RS92 and RS41 indicate that both are dry-biased (in the upper troposphere) and that the RS92 appears more dry-biased than the RS41 indicated in the bottom plot. The dotted lines in the top and middle panels show ± 2 standard errors (from zero) of the combined uncertainties and indicate, respectively, that the CAL radiances for RS92 GDP are statistically inconsistent with IASI

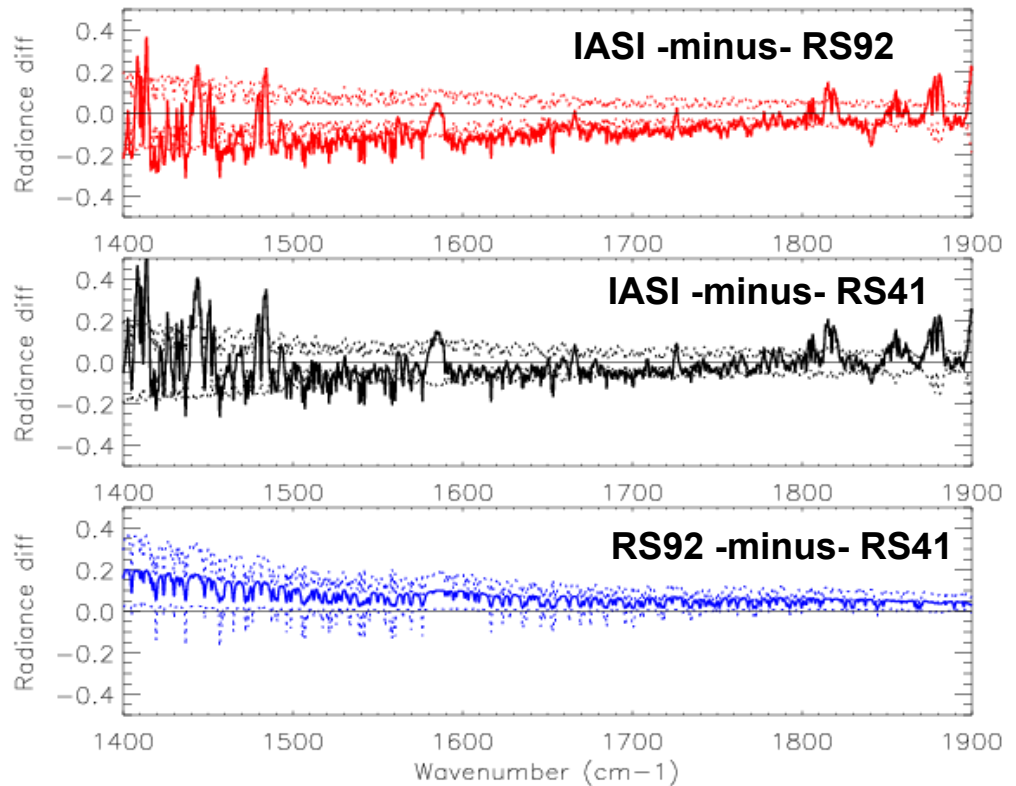


Figure 1. Mean difference (solid curves) between IASI observed and calculated (radiosonde) radiances (OBS – CALC) averaged from 16 daytime cases as described in the text, for Vaisala RS92 (top) and for Vaisala RS41 (middle). Radiance difference units are $\text{mw/m}^2 \text{sr cm}^{-1}$. The lower panel shows the corresponding RS92 minus RS41 differences. In the top and middle panels, dotted lines show ± 2 standard errors (from zero) of the combined uncertainties. If the solid line is usually within the dotted lines, the IASI and radiosonde radiances are generally consistent. In the bottom panel, the dotted lines show ± 2 standard deviations of the RS92 minus RS41 differences from the solid line.

measurements while the CAL radiance for manufacture-processed RS41 appear overall consistent with IASI.

As in Calbet (2017), dry biases are not stated directly in terms of relative humidity (RH) units. Instead, these are estimated by simply adding various RH values to the corresponding radiosonde profiles and re-computing the radiances until the IASI minus RS92 (or RS41) bias becomes negligible. We find from this approach that the daytime upper tropospheric dry RH bias is $\sim 2.5\%$ for RS92 GDP while $\sim 1.5\%$ for RS41 even without GDP developed. The daytime bias in RS92 GDP humidity data obtained from Lauder matches previous Calbet et al. (2017) finding from the

former Nauru DOE Atmospheric Radiation Measurement (ARM) site at the Tropical Western Pacific (TWP).

Analysis of both day and night data from other GRUAN and satellite synchronized sites (not shown) suggests the RS41 dry bias is reduced from daytime to nighttime (by $\sim 1\%$ RH), but available radiosonde collocations with concurrent, cloud-free IASI scenes from those sites are limited.

In summary, daytime upper tropospheric RS41 humidity observations (even without GDP corrections) show an improvement over RS92 data (with GDP corrections) on

the order of 1% RH. The reported RS41 data is found to be consistent with IASI measurements. Data from a longer time period and different geographic sites will be further analyzed to corroborate these results. Fully characterized GDP for RS41 is under development and we plan to repeat the analysis when the product is available.

References

Calbet, X., N. Peinado-Galan, P. Ripodas, T. Trent, R. Dirksen, and M.

Sommer, 2017: Consistency between GRUAN sondes, LBLRTM and IASI. *Atmos. Measur. Tech.*, **10**, 2323-2335, doi:10.5194/amt-10-2323-2017.

Clough, S. A., Shephard, M. W., Mlawer, E. J., Delamere, J. S., Iacono, M. J., Cady-Pereira, K., Boukabara, S., and Brown, R. D., Atmospheric radiative transfer modeling: a summary of the AER codes, *J. Quant. Spectrosc. Ra.*, **91**, 233–244, 2005.

Dirksen, R. J., Sommer, M., Immler, F. J., Hurst, D. F., Kivi, R., and Vömel, H.,

2014: Reference quality upper-air measurements, GRUAN data processing for the Vaisala RS92 radiosonde, *Atmos. Meas. Tech.*, **7**, 4463-4490, doi:10.5194/amt-7-4463-2014.

Immler F.J., J. Dykema, T. Gardiner, D. N. Whiteman, P. W., Thorne, and H. Vömel, 2010: Reference Quality Upper Air Measurements: Guidance for developing GRUAN data products. *Atmos. Meas. Tech.*, **3**, 1217-1231, doi:10.5194/amt-3-1217-2010.

[Discuss the Article](#)

NEWS IN THIS QUARTER

GSICS 20th Executive Panel Meeting (EP-20) held in Sochi, Russia

By Mitch Goldberg (NOAA), Kenneth Holmlund (EUMETSAT), Toshi Kurino (WMO), Lawrence Flynn (NOAA), Manik Bali (NOAA), Dohyeong Kim (KMA), Masaya Takahashi (JMA) and Alexey Rublev (ROSHYDROMET)

Prior to the CGMS-47 meeting, the GSICS Executive Panel (EP) Members from CMA, EUMETSAT, IMD, ISRO, JAXA, JMA, KMA, NASA, NOAA, ROSCOSMOS, ROSHYDROMET, SITP, USGS, WMO (Secretariat), the GCC (Director, Deputy-Director), GDWG (Chair) and GRWG (Chair) convened for the Annual GSICS EP meeting on 16-17 May 2019.

On the agenda were key decisions, endorsements and guidance from the EP on topics related to in-orbit monitoring of meteorological satellites by member agencies. Some of the items that were reported are described below.

The executive panel announced that the European Space Agency (ESA) and the

Shanghai Institute of Technical Physics (SITP) are now full members of the GSICS Executive Panel.

The meeting was kick started by reports from GSICS Executive Panel Chair Mitch Goldberg, GSICS Coordination Center, GSICS Research Working Group and GSICS Data Working Group

The GSICS Coordination Center (GCC) reported that interest in GSICS activities has increased and the quarterly newsletter is subscribed to by over 400 readers world-wide. GSICS EP endorsed a QA4EO based 'GSICS Deliverable' acceptance criteria proposed by GCC and welcomed SSMI

lookup tables as the first GSICS deliverables under the new criteria. GCC received valuable guidance on fine tuning the GPPA to enable faster acceptance and maturity assignment of classical GSICS products generated from newer reference instruments (such as Metop-B and Metop-C IASI and NOAA-20 CrIS) as the current reference instruments, e.g., METOP-A IASI and SNPP-CrIS, complete their mission lives. The GCC provided updates on new features of an Action Tracker, Visualization tools on the GSICS product catalog and reported the publication of four GSICS quarterly newsletter in the past year.



Participants of the GSICS Executive Panel Meeting 2019, Sochi, Russia

The GSICS Research working Group (GRWG) reported calibration results of next generation satellites. These included FY-4A, SLSTR, GOES-16 and NOAA-20 (CrIS and VIIRS) as well as S-NPP. Advances in lunar calibration, Gap filling and AI/Machine Learning and reprocessing have provided new opportunities to collaborate. The Microwave subgroup is working on best practices to use RTMs and NWP models as reference standards in addition to using FCDR's as references. The UV subgroup focused on identifying reference solar spectrum for UV instruments and calibration of spectrometers. The GRWG plans to hold workshops on SI traceable observing systems, Lunar Calibration and Recalibration.

The GSICS Data Working Group (GDWG) provided updates to the EP on three vital tasks undertaken this year. The first was for operations of the collaboration servers that host and share GSICS Products at CMA, NOAA and EUMETSAT. ISRO has established a threads server that is expected to be integrated into the

collaboration server architecture. The second was the GSICS Plotting tool that plots the GSICS products and will soon be upgraded. The third was the agreement on satellite instruments' event logging content among agencies. The GDWG Chair also presented the report on State of Observing System which summarizes the monitoring of instruments of member agencies along with relevant uncertainties. A follow up report on this was presented at the CGMS by the GSICS EP.

Following the Group reports, GPRC reports were presented by all the participating agencies and showed the progress made in using GSICS-formulated best practices in monitoring their instruments, creating FCDR's and ensuring that GSICS reference and transfer targets are exploited to the fullest in achieving high quality instrument monitoring.

The GPRC reports were followed by the state of observing system report presented by Masaya Takahashi, JMA.

The report summarized the performance of instruments across GSICS members in terms of mean bias, standard deviation and time series over the past year.

Manik Bali, GCC informed the EP about two entities to be accepted as GSICS deliverables. These are the SSMI and GPM inter-calibration tables that were provided by Wes Berg, CSU and Racheal Kroodsmma, NASA. Taking the discussion further Scott Hu, CMA presented the progress in generating MW inter-calibration products.

Mitch Goldberg, highlighted steps taken in the integration of GSICS with the WMO Integrated Global Observing System (WIGOS). GSICS also reviewed the High-Level Priority Plan (HLPP) and suggested the inclusion of two new HLPP targets.

GSICS-EP-20 meeting presentation and related documents are available at <http://www.wmo.int/pages/prog/sat/meetings/GSICS-EP-20/GSICS-EP-20.html>

Toshiyuki Kurino Bids Adieu to GSICS

By Manik Bali, GSICS Coordination Center

The GSICS Executive Panel Meeting (EP-20) in Sochi, Russia organized on 16-17 May 2019 was the last GSICS event attended by Toshiyuki Kurino, who retired from WMO on 23 Aug 2019.

Toshi Kurino is one of the founding members of GSICS (since 2005).

Well known to the GSICS community as 'Kurnino San' he is a founder has played a vital role in the growth of GSICS to what it is today. He has also co-chaired the Coordination Group for Meteorological Satellites (CGMS) Working Group II (Satellite Data and Products).

Toshi joined the WMO secretariat in 2016 where he was the Chief of the Space-based Observing System Division. Toshi brought in enormous experience in engaging with the satellite community to GSICS and to the WMO secretariat.

Toshi led the building of the latest version of the OSCAR and the WMO GSICS website. Toshi relentlessly pursued the goals of landing pages and the WMO GSICS WIGOS initiative.

Toshi's guidance to GSICS took GSICS to new heights. At present GSICS has integrated further with the WIGOS system of WMO and groups



such as CEOS and GCOS are actively engaging with the GSICS to achieve the next level of inter-operability.

We wish Toshi all the very best in his future endeavors.

Announcements

COSMIC-2 launched on 25 June 2019

By Shu-Peng (Ben) Ho and Manik Bali, NOAA

Launched in 2006, the Formosa Satellite Mission 3–Constellation Observing System for Meteorology, Ionosphere, and Climate (FORMOSAT-3/COSMIC) has demonstrated the great value of Global Positioning System (GPS) radio occultation (RO) data in weather, climate, and Ionosphere. A COSMIC follow-on constellation, COSMIC-2, blasted into orbit at 2:30 a.m. ET on, June 25, from Cape Canaveral, Florida, aboard a SpaceX Falcon Heavy rocket. COSMIC-2 data will be fed into NOAA's sophisticated numerical weather prediction models to forecast weather and climate and monitor

dynamic changes in Earth's ionosphere, leading to improved weather and space weather forecasts.

COSMIC-2 will produce at least 5,000 high-quality Radio Occultation (RO) profiles daily in the tropics and subtropics.

From a GSICS standpoint the COSMIC-2 missions have become increasingly important in climate monitoring in terms of providing benchmark references for other nadir viewing infrared and microwave sounders on board either polar or geostationary satellites.

Cosmic-2 measurements are of high stability and when used in conjunction with Radiative Transfer Models

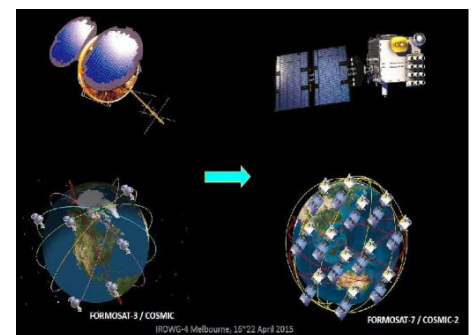


Figure Above shows COSMIC-2 Constellation provide radiances that can be used to monitor satellites at all local times thereby providing opportunities for GSICS-GNSS inter-operability.

GSICS-Related Publications

Chang, T., X. Xiong, and A. Angal. 2019. ‘Terra and Aqua MODIS TEB Intercomparison Using Himawari-8/AHI as Reference’. *Journal of Applied Remote Sensing* 13 (1). <https://doi.org/10.1117/1.JRS.13.017501>

Chu, Mike, and Jennifer Dodd. “Examination of Radiometric Deviations in Bands 29, 31, and 32 of MODIS Collection 6.0 and 6.1.” *Ieee Transactions on Geoscience and Remote Sensing* 57, no. 8 (August 2019): 5790–98. <https://doi.org/10.1109/TGRS.2019.2902399>.

Doelling, D., C. Haney, R. Bhatt, B. Scarino, and A. Gopalan. “The Inter-Calibration of the DSCOVR EPIC Imager with Aqua-MODIS and NPP-VIIRS.” *Remote Sensing* 11, no. 13 (2019). <https://doi.org/10.3390/rs11131609>.

Revel, Charlotte, Vincent Lonjou, Sebastien Marcq, Camille Desjardins, Bertrand Fournie, Celine Coppolani-Delle Luche, Nicolas Guillemot, et al. “Sentinel-2A and 2B Absolute Calibration Monitoring.” *European Journal of Remote Sensing* 52, no. 1 (2019): 122–37. <https://doi.org/10.1080/22797254.2018.1562311>.

Tabata, T., V.O. John, R.A. Roebeling, T. Hewison, and J. Schulz. “Recalibration of over 35 Years of Infrared and Water Vapor Channel Radiances of the JMA Geostationary Satellites.” *Remote Sensing* 11, no. 10 (2019). <https://doi.org/10.3390/rs11101189>

Wang, Likun, and Yong Chen. “Inter-Comparing SNPP and NOAA-20 CrIS Toward Measurement Consistency and Climate Data Records.” *Ieee Journal of Selected Topics in Applied Earth Observations and Remote Sensing* 12, no. 7 (July 2019): 2024–31. <https://doi.org/10.1109/JSTARS.2019.2891701>.

Wilson, T and Xiaoxiong Xiong. “Planning Lunar Observations for Satellite Missions in Low-Earth Orbit.” *Journal of Applied Remote Sensing* 13, no. 2 (May 9, 2019): 024513. <https://doi.org/10.1117/1.JRS.13.024513>.

Xu, H. 2019. ‘Cross-Track Infrared Sounder Spectral Gap Filling Toward Improving Intercalibration Uncertainties’. *IEEE Trans. Geosc. Remote Sens.* 57 (1): 509–19. <https://doi.org/10.1109/TGRS.2018.2857833>.

Zhi, Dandan, Wei Wei, Yanna Zhang, Tanqi Yu, Yan Pan, Ling Sun, Xin Li, and Xiaobing Zheng. “FengYun-3 B Satellite Medium Resolution Spectral Imager Visible On-Board Calibrator Radiometric Output Degradation Analysis.” *Ieee Transactions on Geoscience and Remote Sensing* 57, no. 6 (June 2019): 3240–51. <https://doi.org/10.1109/TGRS.2018.2882858>

Submitting Articles to the GSICS Quarterly Newsletter:

The GSICS Quarterly Press Crew is looking for short articles (800 to 900 words with one or two key, simple illustrations), especially related to calibration / validation capabilities and how they have been used to positively impact weather and climate products. Unsolicited articles may be submitted for consideration anytime, and if accepted, will be published in the next available newsletter issue after approval / editing. Please send articles to manik.bali@noaa.gov.

With Help from our friends:

The GSICS Quarterly Editor would like to thank Tim Hewison (EUMETSAT), Sebastien Wagner (EUMETSAT) and Lawrence E Flynn (NOAA) for reviewing articles in this issue.

GSICS Newsletter Editorial Board

Manik Bali, Editor
Lawrence E. Flynn, Reviewer
Lori K. Brown, Tech Support
Fangfang Yu, US Correspondent.
Tim Hewison, European Correspondent
Yuan Li, Asian Correspondent

Published By

GSICS Coordination Center
NOAA/NESDIS/STAR NOAA
Center for Weather and Climate Prediction,
5830 University Research Court
College Park, MD 20740, USA

Disclaimer: The scientific results and conclusions, as well as any views or opinions expressed herein, are those of the authors and do not necessarily reflect the views of NOAA or the Department of Commerce or other GSICS member agencies.